Aus der Abteilung Experimentelle und Klinische Toxikologie
Universität des Saarlandes
Homburg/Saar
Leiter: Prof. Dr. Dr. h.c. Hans H. Maurer

New cathinone-derived designer drugs 3-bromomethcathinone and 3-fluoromethcathinone: studies on their metabolism in rat urine and human liver microsomes using GC-MS and LC-high-resolution MS and their detectability in urine

Dissertation zur Erlangung des Grades eines Doktors der Medizin
der Medizinischen Fakultät der UNIVERSITÄT DES SAARLANDES

2012

vorgelegt von

Christian Vollmar

geboren am 29.11.1985 in Zweibrücken

Teile dieser Doktorarbeit sind Gegenstand folgender Publikation:

M. R. Meyer, **C. Vollmar**, A. E. Schwaninger, and H. H. Maurer:
New cathinone-derived designer drugs 3-bromomethcathinone and 3-fluoromethcathinone: studies on their metabolism in rat urine and human liver microsomes using GC-MS and LC-high-resolution MS and their detectability in urine:
J Mass Spectrom, 2012:47, 253-262

Table of contents

1 ZUSAMMENFASSUNG

3-Bromomethcathinon (3-BMC) und 3-Fluoromethcathinon (3-FMC) sind zwei neue Designerdrogen die zu den Neuerscheinungen der letzten Jahre auf dem weltweiten Drogenmarkt zählen und u.a. 2009 in Israel beschlagnahmt wurden. Beide Substanzen finden Verwendung als sogenannte „Recreational Drugs“, können über das Internet als sogenannte „Badesalze“ oder „Düngemittel“ bezogen werden und traten auch in Deutschland auf.

Ziel dieser Studie ist die Identifizierung der Phase I und Phase II Metabolite in Rattenurin sowie menschlichen Lebermikrosomen unter Verwendung von Gaschromatographie-Massenspektrometrie (GC-MS) oder Flüssig-Chromatographie-Hochauflösender-Massenspektrometrie (LC-HRMS) Techniken. Nach Extraktion der Urinproben, jeweils mit und ohne Konjugatspaltung, erfolgte die Auftrennung und Identifikation der Metaboliten mittels GC-MS und LC-HRMS. Die nachgewiesenen Hauptschritte im Stoffwechsel waren demnach die *N*-Demethylierung, die Reduktion der Ketogruppe zum korrespondierenden Alkohol, die Hydroxylierung des aromatischen Ringsystems und Kombinationen dieser Schritte. Bezüglich 3-Bromomethcathinon war *N*-Demethyl-dihydro-3-bromomethcathinon der Hauptmetabolit *in vivo*, für 3-Fluoromethcathinon waren dies Hydroxy-3-fluoromethcathinon und *N*-Demethyl-dihydro-3-fluoromethcathinon. Die Elementarzusammensetzung der identifizierten Metabolite wurden mittels LC-HRMS verifiziert. Auch wurden die korrespondierenden Phase II Metaboliten unter Verwendung der LC-HRMS identifiziert.

Die beiden Substanzen konnten in der sogenannten „Systematisch toxikologischen Analyse“ (STA) - nach Verabreichung einer von Konsumenten vermutlich gebräuchlichen Dosis an die Ratten - im Urin nachgewiesen werden.

Schlussendlich war ein weiteres Ziel dieser Arbeit die Identifizierung der menschlichen Cytochrom P450 Isoenzyme, welche die wichtigsten Stoffwechselschritte katalysieren. Dies ermöglicht Schlussfolgerungen bezüglich Medikamenteninteraktionen oder genetischen Variationen, die für Konsumenten von Stoffgemischen, welche diese Designerdrogen enthalten, von Bedeutung sein können. Den Cytochrom P-450 (CYP) Enzym-basierten Kinetikstudien zufolge war CYP2B6 für die *N*-Demethylierung von sowohl 3-Bromomethcathinon als auch von 3-Fluoromethcathinon das *in vivo* wichtigste Enzym.

2 SUMMARY

Among the substances of abuse that appeared during the last years on the worldwide drug market are 3-bromomethcathinone (3-BMC) and 3-fluoromethcathinone (3-FMC), two new designer drugs, which were seized 2009 in Israel among others. Both substances, used as recreational drugs, can be purchased online as so called “bath salts” or “plant feeders” and appeared also in Germany. The aim of the presented study was to identify the 3-BMC and 3-FMC phase I and phase II metabolites in rat urine and human liver microsomes using gas chromatography-mass spectrometry (GC-MS) or liquid chromatography-high resolution mass spectrometry (LC-HRMS) techniques. Rat urine samples were extracted with and without enzymatic cleavage of the conjugates. Separation and identification of the metabolites was executed via GC-MS and LC-HRMS. The main metabolic steps were *N*-demethylation, reduction of the keto group to the corresponding alcohol, hydroxylation of the aromatic system and combinations of these steps. For 3-BMC, the main *in vivo* metabolites were *N*-demethyl-dihydro-3-BMC, for 3-FMC hydroxy-3-FMC and *N*-demethyl-dihydro-3-FMC. LC-HRMS verified the elemental composition of the metabolites postulated by GC-MS interpretation. The corresponding Phase II metabolites were also identified using the LC-HRMS analysis approach. Additionally, both compounds could be detected according to the standard systematic toxicological analysis (STA) in rat urine after administration of a suspected recreational dose to rats.

Another aim was the identification of the human cytochrome P450 (CYP) isoenzymes catalyzing the main metabolic step allowing conclusions on drug-drug interactions or genetic variations gathering importance for humans consuming drugs containing these designer drugs. According to the CYP enzyme kinetic studies, CYP2B6 was the most relevant enzyme for both the *N*-demethylation of 3-BMC and 3-FMC.

3 INTRODUCTION

In recent years, many new substances appeared on the drugs of abuse market. Among these compounds were new cathinone derivates that are synthesized and sold via the internet to a worldwide customer base as so called new "legal highs", declared as "plant feeders" or "bath salts".

The added ingredients of the compounds sold online are caffeine, lidocaine, procaine, or often even unknown [1].

Another problem is the use of trivial names for these substances of abuse, so called "street names", leading to the risk of misinterpretation because of names sounding too similar, e.g. "Mephedrone" (4-Methylmethcathinone), "Methedrone" (4-Methoxymethcathinone), "Flephedrone" (4-Fluoromethcathinone) or "Fluphedrone" (3-Fluoromethcathinone) [2].

Last but not least, due to the fact that the producers can not be controlled and are not subject of any restriction, ingredients get replaced or new agents are added but the compound is still sold under the identical name, as it is discussed in several online forums, e.g. for the compound "charge+" that will also be discussed later because of its agent 3-FMC [3].

In conclusion, the risks for health and possible addiction can not be estimated and seem to be very high as, in the worst case, a recreational user of these online-sold drugs of abuse is consuming an unknown amount of a compound of unknown main agent with unknown added substances.

In 2009, several of these psychoactive substances were seized by the Israeli police, among others 3-BMC and 3-FMC (fluphedrone). Samples were sent to our institute with request for further research.

3.1 Chemical characterization of 3-BMC and 3-FMC

3-BMC and 3-FMC are synthetic derivates of cathinone, a natural stimulant with effects similar to amphetamine, which can be synthesized and also extracted from fresh leaves of *Catha Edulis* [4].

The only difference concerning the chemical structure of both substances lies within the different ring-substituting heteroatom in ring position three, which is bromine in the case of 3-BMC and fluorine for 3-FMC as depicted in Fig. 1.

As these substances are cathinone derivates, a characteristic keto-group can be found in beta position. The alpha carbon is the chiral center of the two analytes.

The molecular formula for 3-BMC is $C_{10}H_{12}BrNO$ with a nominal molecular mass of 242 g/mol, according to the natural appearance of the two isotopes ^{79}Br, accounting for 50.69% and ^{81}Br, making up 49.31% of the natural bromine appearance, leading to a molecular weight of 241 Da or 243 Da, respectively. The IUPAC name of 3-BMC is 1-(3-bromophenyl)-2-(methylamino)propan-1-one.

Concerning 3-FMC, the molecular formula is $C_{10}H_{12}FNO$ with a nominal molecular mass of 181 g/mol and 1-(3-fluorophenyl)-2-(methylamino)propan-1-one as IUPAC name.

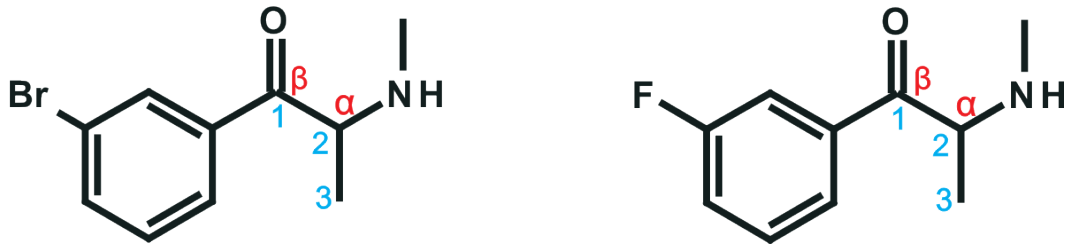

Figure 1. Chemical structure of 3-bromomethcathinone (left) and 3-fluoromethcathinone (right); numbering according to the IUPAC nomenclature (blue), alpha-beta numbering in relation to functional group (red)

3.2 Effects of 3-BMC and 3-FMC

Except for 3-BMC, for which was shown to act as a serotonin and norepinephrine reuptake inhibitor [5] with more intense antidepressant than stimulating properties [6], there is no scientific knowledge about the effects of 3-BMC and 3-FMC on the human organism after consumption.

Due to their chemical similarity to mephedrone (4-methylmethcathinone), the most popular of the cathinone derivates [7], and according to users' reports found in online forums, both should cause similar stimulant and empathogenic effects as mephedrone [8].

In a study published by Winstock *et al.* [9], mephedrone consumers indicated the most prevalent effects: increased energy, euphoria, talkativeness, urge to move and do things, empathy, bruxism, body sweats, no appetite for food, heart racing, feeling restless or anxious, increased sexual desire, forgetting things, overheating, tremor in extremities, blurred vision and improved concentration. Described withdrawal effects were tiredness, insomnia at end of session, nasal congestion, inability to concentrate, irritability, lost memory of mephedrone session, depression, being in an emotional state and anxiety.

Trip reports which can be found in numerous online forums revealed that 3-BMC and 3-FMC seem to be consumed orally, smoked, nasal inhaled or injected intravenously [8].

These compounds are scheduled in Israel, Australia, New Zealand and other countries, but not in Germany (so far -03/2012).

They are still available via the internet, e.g. as part of a compound named "Charge+" or as agent in capsules named "Lift", "Sub Coca Dragon", "High Spirit" or "Neo Dove 2" [2,10].

Fig. 2 shows pictures of "Charge+" and "Lift", two recreational drugs whose main agent is 3-FMC.

Figure 2. Seized "Charge+" (left) and online bought capsules called "Lift" (right); both containing 3-FMC

3.3 Former publications on 3-BMC and 3-FMC

As mentioned above, 3-BMC was already object of research in a study showing 3-BMC's ability to inhibit the reuptake of serotonin and norepinephrine by Foley and Cozzi [5, 6].

Archer published GC-MS and NMR data on the three fluoromethcathinone isomers 2-FMC, 3-FMC and 4-FMC. He identified 3-FMC as the agent of "Lift", "Sub Coca Dragon", "High Spirit" and "Neo Dove 2" by using the NMR technique which is able to distinguish between the three isomers because of differences in the values in the aromatic region of the ^{1}H NMR spectra whereas the GC-MS technique was not able to differentiate the isomers due to similar fragmentation and retention times [2].

Westpfahl *et al.* presented GC-MS data of 3-FMC and some of its derivatives as well as NMR

data by analyzing and identifying 3-FMC as main agent of an in 2009 in Baden Württemberg (Germany) seized compound named "Charge+" [10].

A Phase I metabolism study was operated by Pawlik *et al.* using rabbit liver slices, indicating *N*-demethylation and ring-hydroxylation as the first metabolic steps [11].

3.4 Aim of the present work

In clinical and forensic toxicology, screening for and determination of drugs (of abuse) is an important task. Sophisticated general screening procedures allow detection of a series of drug classes in one step [12,13].

The aim of this study was to identify the phase I and phase II metabolites of 3-BMC and 3-FMC in rat urine as well as in human liver microsomes by GC-MS and LC-HRMS.

Additionally, the aim of the work was to identify the human CYP isoenzymes responsible for the main metabolic steps of these compounds.

Finally, targets for detectability and identification of 3-BMC and 3-FMC in urine by the standard systematic toxicological analysis (STA) using GC-MS or LC-MS^n should be defined to detect an intake of 3-BMC and 3-FMC.

4 EXPERIMENTAL PROCEDURES / MATERIAL AND METHODS

4.1 Chemicals and reagents

3-BMC and 3-FMC were provided by the analytical laboratory oft he DIFS Israel Police for research purposes. Isolute HCX cartridges (130 mg, 3 mL) were obtained from Biotage (Uppsala, Sweden). $NADP^+$ was obtained from Biomol (Hamburg, Germany), and isocitrate and isocitrate dehydrogenase from Sigma (Taufkirchen, Germany). All other chemicals and reagents were obtained from E. Merck, Darmstadt (Germany) and were of analytical grade. The following microsomes were from Gentest and delivered by NatuTec (Frankfurt/Main, Germany): baculovirus-infected insect cell microsomes (Supersomes), containing 1 nmol/mL of human cDNA-expressed CYP1A2, CYP2A6, CYP2B6, CYP2C8, CYP2C9, CYP2C19, CYP2D6, CYP2E1 (2 nmol/mL), CYP3A4, or CYP3A5 and pooled human liver microsomes (pHLM, 20 mg microsomal protein/mL, 400 pmol total CYP/mg protein). After delivery, the microsomes were thawed at 37°C, aliquoted, snap-frozen in liquid nitrogen, and stored at -80°C until use.

4.2 Urine samples

The investigations were performed using urine of male rats (Wistar, Charles River, Sulzfleck, Germany) for toxicological diagnostic reasons according to the corresponding German law (http://www.gesetze-im-internet.de/tierschg/). They were administered in an aqueous suspension by gastric intubation of a single 20mg/kg body mass dose of 3-BMC or 3-FMC for identification oft the metabolites and a single 1 mg/kg body mass dose each for toxicological analysis. The rats were housed in metabolism cages for 24 h, having water *ad libitum*. Urine was collected separately from the faeces over a 24-h period. All samples were directly analyzed and then stored at -20°C. Blank urine samples were collected before drug administration to check whether the samples were free of interfering compounds.

4.3 Sample preparation

4.3.1 Sample preparation for identification of phase I metabolites by GC-MS and LC-HRMS

A 2.5 mL portion of urine was adjusted to pH 5.2 with acetic acid (1 M, approximately 50 µl) and incubated at 56°C for 1.5 h with 50 µl of a mixture (100 000 Fishman units/mL) of glucuronidase (EC No. 3.2.1.31, E. Merck, Darmstadt, Germany) and arylsulfatase (EC No.

3.1.6.1, E. Merck, Darmstadt, Germany), from *Helix Pomatia* L. The urine sample was then diluted with 2.5 mL of water and loaded on a HCX cartridge, previously conditioned with 1 mL of methanol and 1 mL of water. After passage of the sample, the cartridge was washed with 1 mL of water, 1 mL of 0.01 M hydrochloric acid, and again with 1 mL of water. The retained non-basic compounds were first eluted into a 1.5 mL reaction vial with 1 mL of methanol (fraction 1), whereas the basic compounds were eluted in a second step into a different vial with 1 mL of a freshly prepared mixture of methanol/aqueous ammonia 32% (98:2 v/v, fraction 2). The eluates were gently evaporated to dryness under a stream of nitrogen at 56°C and reconstituted in 50 µL of acetonitrile for LC-HRMS. A 10 µL aliquot was injected into the LC (only underivatized) or 1 µL into GC.

4.3.2 Sample preparation for identification of phase II metabolites by HR-ESI-MS

For elucidating the formation of glucuronides and sulfates, 200 µL of urine was mixed with 200 µL of acetonitrile for protein precipitation, centrifuged at *14.000g* for 5 min and the supernatant was transferred into an autosampler vial. A 10 µL aliquot of this solution was injected into the LC system.

4.3.3 Sample preparation for systematic toxicological analysis (STA) by GC-MS

Systematic toxicological analysis procedure (hydrolysis, extraction and microwave-assisted acetylation) for urine was used according to published procedures [12,14]. Briefly, the samples (5 mL) were divided into two aliquots, and one part was submitted to acid hydrolysis. Thereafter, the sample was adjusted to pH 8-9 and the other aliquot of untreated urine was added. This mixture was extracted with a dichloromethane-isopropanol-ethyl acetate mixture (1:1:3 v/v/v) and the organic layer was evaporated to dryness. The residue was acetylated with an acetic anhydride-pyridine mixture under microwave irradiation. After evaporation of the derivatization mixture, the residue was dissolved in 100 µL of methanol, and 2 µL was injected into the GC-MS system.

4.4 Enzymatic Part

4.4.1 Microsomal Incubations

Microsomal incubations were performed at 37°C with 250 µM 3-BMC/3-FMC with CYP1A2, CYP2A6, CYP2B6, CYP2C8, CYP2C9, CYP2C19, CYP2D6, CYP2E1, CYP3A4, or CYP3A5 for 30 min. Besides enzymes and substrate, incubation mixtures (final volume: 50 µL) consisted of 90 mM phosphate buffer (pH 7.4), 5 mM Mg^{2+}, 5 mM isocitrate, 1.2 mM $NADP^{+}$, 0.5 U/mL isocitrate dehydrogenase, and 200 U/mL superoxide dismutase. For incubations with CYP2A6 or CYP2C9, phosphate buffer was replaced with 45 mM and 90 mM Tris-buffer, respectively, according to the Gentest manual. Reactions were started by addition of the ice-cold microsomes and stopped with 50 µL of an ice-cold mixture of acetonitrile with 0.1% formic acid, containing the internal standard (metamfepramone, 10 µM). The solution was centrifuged for 2 min at 14000 *g*, 50 µL oft he supernatant phase was transferred to an autosampler vial and injected into the LC-HRMS apparatus for analysis, and LC-HRMS conditions were chosen as described below.

4.4.2 Initial screening studies

Incubations were performed with 250 µM of 3-BMC or 3-FMC and 50 pmol/mL of CYP1A2, CYP2A6, CYP2B6, CYP2C8, CYP2C9, CYP2C19, CYP2D6, CYP2E1, CYP3A4, or CYP3A5 for 60 min.

4.4.3 Kinetic studies

Kinetic constants of *N*-demethylation were derived from incubations with an incubation time of 10 min 30 pmol/mL (P450s) protein concentration. Incubation time and enzyme concentration were chosen to be within a linear range of metabolite formation. The substrate concentrations were used as provided in Table 1.

Enzyme kinetic constants were estimated by non-linear curve-fitting using GraphPad Prism 5.00 software (San Diego, CA). The Michaelis-Menten equation (Eqn (1)) was used to calculate apparent K_m and V_{max} values for single-enzyme systems.

$$V = \frac{V_{\max} \times [S]}{K_m + [S]} \quad (1)$$

Eadie-Hofstee plots were used to check for biphasic kinetics [15]. If the Eadie-Hofstee plot indicated biphasic kinetics, equation (1) and the alternative equation (2) for a two site binding model were applied to the respective data. If equation (2) was found to fit the data significantly better (F-test, $p < 0.05$), biphasic kinetics were assumed.

$$V = \frac{V_{\max,1} \times [S]}{K_{m,1} + [S]} + \frac{V_{\max,2} \times [S]}{K_{m,2} + [S]} \quad (2)$$

Table 1. Substrate concentrations used for microsomal incubations [µM]

3-FMC			3-BMC	
CYP2B6	CYP2D6	CYP2C19	CYP2B6	CYP2D6
25	1	1	75	1
75	10	10	125	10
125	25	75	250	25
250	75	125	500	75
500	125	250	750	125
750	250	500	1000	250
1000	500	750	1500	500
1500	750	1000		
	1000			
	1500			

4.4.4 Calculation of relative activity factors, contributions, and percentages of net clearance

The relative activity factor (RAF) approach [16-18] was used to account for differences in functional levels of redox partners between the two enzyme sources. The turnover rates (TR) of CYP2C19 (probe substrate (PS) *S*-mephenytoin), CYP2D6 (PS bufuralol) and CYP2B6 (PS 7-ethoxy-4-trifluoromethylcoumarin) in insect cell microsomes (ICM) and HLM were taken from the supplier's data sheets. The RAFs were calculated according to equation (3).

$$RAF_{enzyme} = \frac{TR_{PS} \text{ in HLM}}{TR_{PS} \text{ in ICM}} \quad (3)$$

The enzyme velocities V_{enyzme} (see equation (1)) for the respective metabolic reactions were calculated at different substrate concentrations and were then multiplied with the corresponding RAF leading to a value, which is defined as 'contribution'. The V_{max} and the K_m values (equation (1)) were obtained from the incubations with cDNA-expressed P450s.

$$contribution_{enzyme} = RAF_{enzyme} \times V_{enzyme} \quad (4)$$

From these corrected activities (contributions) the percentages of net clearance by a particular P450 at a certain substrate concentration can be calculated according to equation (5):

$$clearance_{enyzme}[\%] = \frac{contribution_{enyzme}}{\sum contribution_{enzyme}} \times 100 \quad (5)$$

4.5 GC-MS / LC-HRMS settings

4.5.1 GC-MS apparatus for identification oft the Phase I metabolites

The extracts were analyzed using a Hewlett Packard (HP, Agilent, Waldbronn, Germany) 5890 Series II GC combined with an HP 5972 MSD mass spectrometer and an HP MS ChemStation (DOS series) with HP G1034C software Version C03.00. The GC conditions were as follows: splitless injection mode; column, HP-1 capillary (12m x 0.2mm I.D.), cross-linked methyl silicone, 330 nm film thickness; injection port temperature, 280 °C; carrier gas, helium; flow rate, 1 mL/min; column temperature, programmed from 100 °C to 310 °C at 15 °/min, initial time 3 min, final time 8 min. The MS conditions were as follows: full-scan mode, *m/z* 50-550 u; EI mode, ionization energy, 70 eV; ion source temperature, 220 °C; capillary direct interface, heated at 280 °C.

4.5.2 GC-MS apparatus and procedure for STA

An HP 5890 Series II gas chromatograph combined with an HP 5972A MSD mass spectrometer was used. The GC conditions were the same as fort he metabolism studies with the exception of temperature, which was programmed from 100 °C to 310 °C at 30 °/min. The

MS conditions were as follows: full-scan mode, *m/z* 50-550 u; EI mode, ionization energy, 70 eV; ion source temperature, 220 °C; capillary direct interface, heated at 260 °C.

For toxicological detection of acetylated drugs and their metabolites, mass chromatography was used with the selected ions *m/z* 58, 86, and 183 for 3-BMC and *m/z* 58, 86, 95, and 123 for 3-FMC. Generation of the mass chromatograms could be started by clicking the corresponding pull-down menu, which executes the user-defined macros [12,13,19]. The identity of the peaks in the mass chromatograms was confirmed by computerized comparison of the mass spectra underlying the peaks (after background subtraction) with reference spectra recorded during this study [20].

In addition, the full-scan data files acquired by the GC-MS system were evaluated by automated mass spectral deconvolution and identification system (AMDIS) (http://chemdata.nist.gov/mass-spc/amdis/) in simple mode. The used target library was a modified version of the Maurer/Pfleger/Weber MPW_2011 library [20], from which all mass spectra of silylated and perfluoroacetylated compounds had been eliminated and the spectra of (acetylated) 3-BMC and 3-FMC and its metabolites were added using the "build one library" option contained in the AMDIS main program. According to Meyer *et al.* [19], the used deconvolution parameter settings were as follows: width 32, adjacent peak subtraction two, resolution high, sensitivity very high, and shape requirements low. The minimum match factor was set to 50.

4.5.3 LC-HRMS apparatus for identification of Phase I and II metabolites and for microsomal incubations

3-BMC, 3-FMC and their metabolites were analyzed using a ThermoFisher Scientific (TF, Dreieich, Germany) Accela LC system consisting of a degasser, a quaternary pump and a HTC PAL autosampler (CTC Analytics AG, Zwingen, Switzerland), coupled to a TF Exactive system equipped with a heated electrospray ionization II source. The LC conditions were as follows: Grace Davis Discovery Science (Waukegan, Il) C18/cation exchange column (150mm x 4.6 mm, 5 µM) and gradient elution with 50 mM aqueous ammonium formate buffer containing 0.1% (V/v) formic acid as Mobile Phase A and acetonitrile containing 0.1% (v/v) formic acid as mobile Phase B. The gradient and flow rate were programmed as follows: 0-4 min 98% A to 40% A at 500 µL/min, 4-7 min hold 10% A at 1000 µL/min and 7-10 min hold 98% A at 750 µL/min. Injection volume was 10 µL.

The MS conditions were as follows: positive scan mode from *m/z* 50 to 800 (MS [1], resolution 100 000 at 1 Hz) sheath gas, nitrogen at a flow rate of 18 AU; heater temperature,

350 °C; spray voltage, 4.00 kV; ion transfer capillary temperature, 250 °C; capillary voltage, 25 V; tube lens voltage, 85 V; skimmer voltage, 22 V; maximum injection time, 250 ms; Higher-energy collision dissociation (HCD) at 25 eV (MS [2], positive scan mode from *m/z* 50 to 1000, resolution 50 000 at 2 Hz). The instrument was mass calibrated prior to analysis infusing a Positive Mode Cal Mix provided by Supelco (Bellefonte, PA) at a flow rate of 5 µL/min using a syringe pump.

5 RESULTS AND DISCUSSION

5.1 Identification of the Phase I metabolites by GC-MS

The urinary metabolites of the substances were identified by full-scan EI MS after GC separation. The postulated structures of the metabolites were deduced from the fragments detected in the EI mode, which were interpreted in correlation to those of the parent compound according to the fragmentation rules described by, e.g. McLafferty and Turecek and Smith and Bush [21-23]. The gas chromatographic retention indices (RI) were determined according to de-Zeeuw *et al* [24]. Structures and predominant fragmentation patterns of 3-BMC (Mass Spectrum 1) as well as of its acetylated metabolites are shown in Fig. 3; those of 3-FMC (Mass Spectrum 1) are shown in Fig. 4(a) and 4(b).

In the following, important fragmentation patterns of the EI mass Spectra of 3-BMC, 3-FMC and their derivatized metabolites will be discussed in relation to the postulated metabolite structures depicted in Fig. 3 for 3-BMC and Fig. 4(a) and 4(b) for 3-FMC. The numbers of the corresponding mass spectra are given in brackets.

5.1.1 3-Bromomethcathinone

The underivatized and the acetylated spectra of 3-BMC and 3-FMC show several similarities, assumed due to their structural similarity illustrated in the introduction part of this work.

Cleavage between Position 1 and 2 leads to the immonium ion *m/z* 58, represented by the base peak in the spectrum of 3-BMC (Fig. 3, no. 1). There was also a strong peak of *m/z* 56, which was described by Archer appearing also in a pyrolysis product upon injection [2]. The bromophenyl and the bromobenzyl-oxy ions are represented by the signals at *m/z* 155/157 and *m/z* 183/185, respectively. The benzyl ring is represented by the *m/z* 76 (Spectra 1, 2 and 3) or *m/z* 77 (Spectrum 4), depending on the moiety in the beta position. In the spectrum of acetylated 3-BMC, a base peak of *m/z* 58 and an abundant *m/z* 100 represent the imminium

part of the molecule, and the unchanged bromobenzyl-oxo moiety is represented by the ions at *m/z* 76, 155/157 and 183/185.

However, most metabolite spectra contained an *m/z* 86 base peak, resulting from *N*-demethylation and derivatization by acetylation. Spectra 4 and 5 show a shift of *m/z* 59 (*m/z* 313/315 to 254/256 and *m/z* 371/373 to 312/314) as a result of a loss of acetic acid in beta position, which is in line with the fragmentation patterns. Spectrum 4 shows signals at *m/z* 77, 155/157 and 183/185, indicating an unchanged bromophenyl moiety; hence, the loss of acetic acid can be explained by a reduced and acetylated beta-keto moiety.

According to Spectrum 5, it can be deduced that these compounds contain, besides a reduced beta-keto moiety, a hydroxyl group in the aromatic ring system. Alpha cleavage leads to *m/z* 285/287 and finally to *m/z* 201/203 and *m/z* 241/243 induced by a twice loss of an acetyl group bound to a hydroxyl moiety (shift of *m/z* 42).

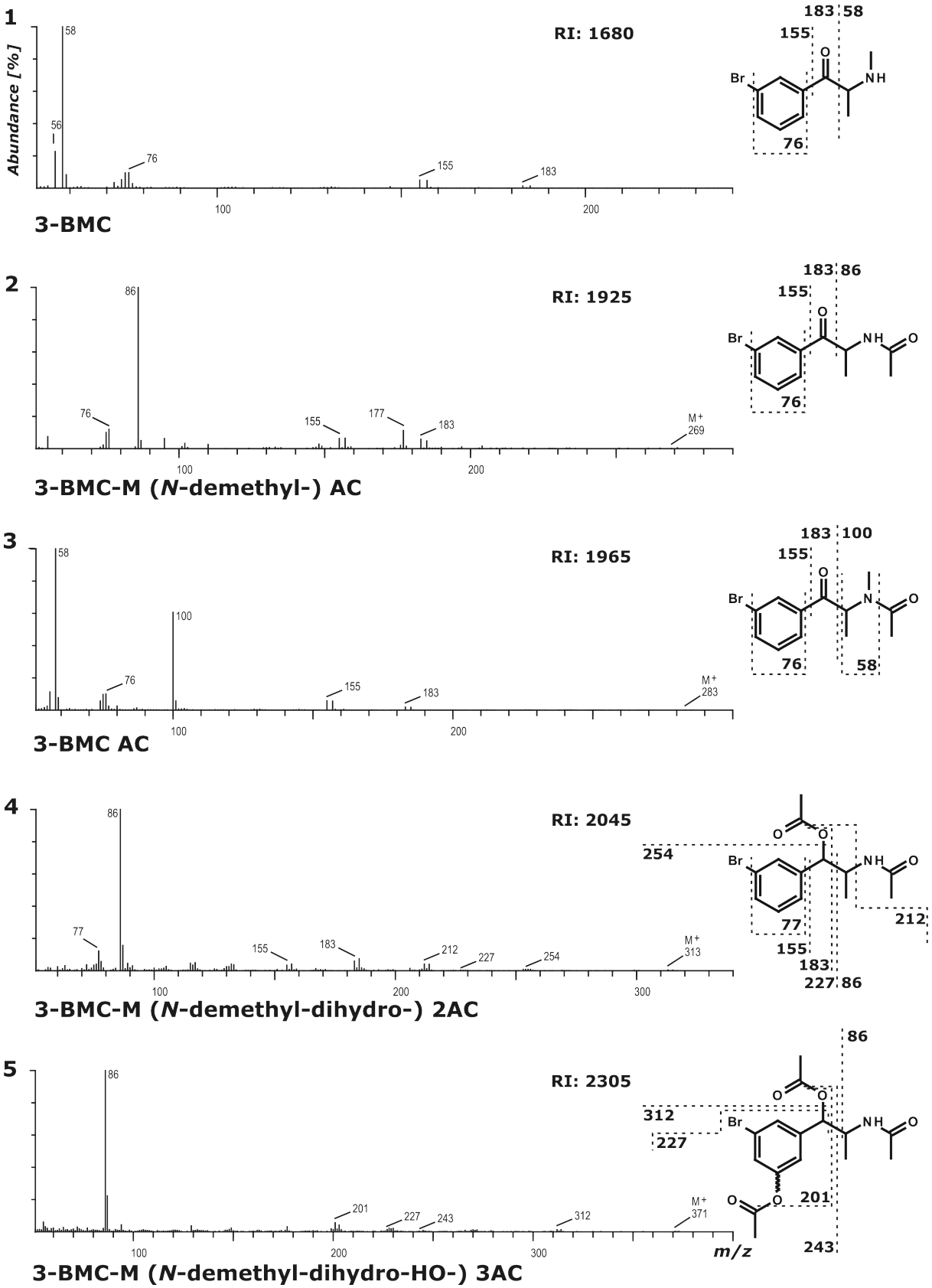

Figure 3. EI mass spectra, gas chromatographic retention indices (RI), proposed structures and predominant fragmentation patterns of 3-BMC and its metabolites arranged according to their RI.

5.1.2 3-Fluoromethcathinone

The EI spectrum of the underivatized 3-FMC was identical to the spectrum recorded by Archer [2] (Fig. 4 (a), spectrum 1). Alpha cleavage between position 1 and 2 results in an immonium ion *m/z* 58 representing the base peak of the spectrum. As discussed for 3-BMC, an ion *m/z* 56 was also observed in the mass chromatogram of 3-FMC. Further prominent ions are the fluorophenyl cation at *m/z* 95 and the fluorobenzyloxy cation at *m/z* 123. After a phenyl bond cleavage, an ion at *m/z* 109 is formed [25]. In analogy to the underivatized compound, the spectrum of the acetylated 3-FMC (Fig. 4(a), no. 3) contains the ions *m/z* 75, 95 and 123. The alpha cleavage between Position 1 and 2 forms an imminium ion *m/z* 100; this *m/z* 100 ion forms after loss of the acetyl moiety the imminium ion *m/z* 58, which also represents the base peak of the spectrum. Cleavage of the acetyl moiety forms the ion at *m/z* 180, and fortunately the $M^{+\cdot}$ ion *m/z* 223 is more dominant than in the spectrum of the parent compound. It can be concluded that the ions *m/z* 100 and 58 represent an unchanged acetyl immonium moiety, as presented in Spectra 3 (Fig. 4 (a)) and 6, 7, 8, 9 (Fig. 4 (b)).

Spectra 7, 8 and 9 in Fig. 4(b) show signals at *m/z* 111 and 139. The shift of 16 units (*m/z* 95 to 111 and *m/z* 123 to 139) indicates the introduction of a hydroxyl group in the fluorophenyl moiety. The exact position of the hydroxyl group cannot be deduced from the fragmentation patterns. According to RI and the fragmentation patterns, it can be concluded that the metabolite represented in Spectrum 7 (Fig. 4 (b)) contains a free hydroxyl group, whereas there is an acetylated hydroxyl group at the fluorophenyl moiety of spectrum 8 (Fig. 4 (b)), leading to a $M^{+\cdot}$ of *m/z* 281 with a shift of 43 (*m/z* 281 to 238) in Spectrum 8 (Fig. 4 (b)).

According to spectra 4, 5 (Fig. 4 (a)), 6 and 9 (Fig. 4 (b)) it can be deduced that the beta-keto group was reduced to a hydroxyl moiety, which has been derivatized by acetylation. This results in a shift of 59 (*m/z* 253 to 194 in spectra 4 and 5 (Fig. 4 (a)); to *m/z* 208 in spectrum 6 (Fig. 4 (b))) and a shift of 101 (to *m/z* 224 in spectrum 9 (Fig. 4 (b))) caused by elimination of acetic acid (*m/z* 59 and an additional acetyl group (*m/z* 42). This metabolic reaction also introduces a further chiral center at the beta carbon, leading to diastereomers represented by two signals with spectra 4 and 5 (Fig. 4 (b)).

Metabolites represented by spectra 6 and 9 (Fig. 4 (b)) were only detected once probably due to their very low abundance or insufficient separation. However, it is not possible to determine which diastereomer belongs to which spectrum according to the fragmentation patterns. Alpha cleavage between position 1 and 2 leads to an ion of *m/z* 166 in spectra 4, 5 (Fig. 4 (a)) and 6 (Fig. 4 (b)), and the abundant *m/z* 86 in spectra 2,4 and 5 (Fig. 4 (a)) is a consequence of *N*-demethylation and acetylation. The ion at *m/z* 152 is also a consequence of

this *N*-acetyl moiety, as recognized in spectrum 2 (Fig. 4 (a)) and in a combination with the loss of acetic acid in spectra 4 and 5 (Fig. 4 (a)).

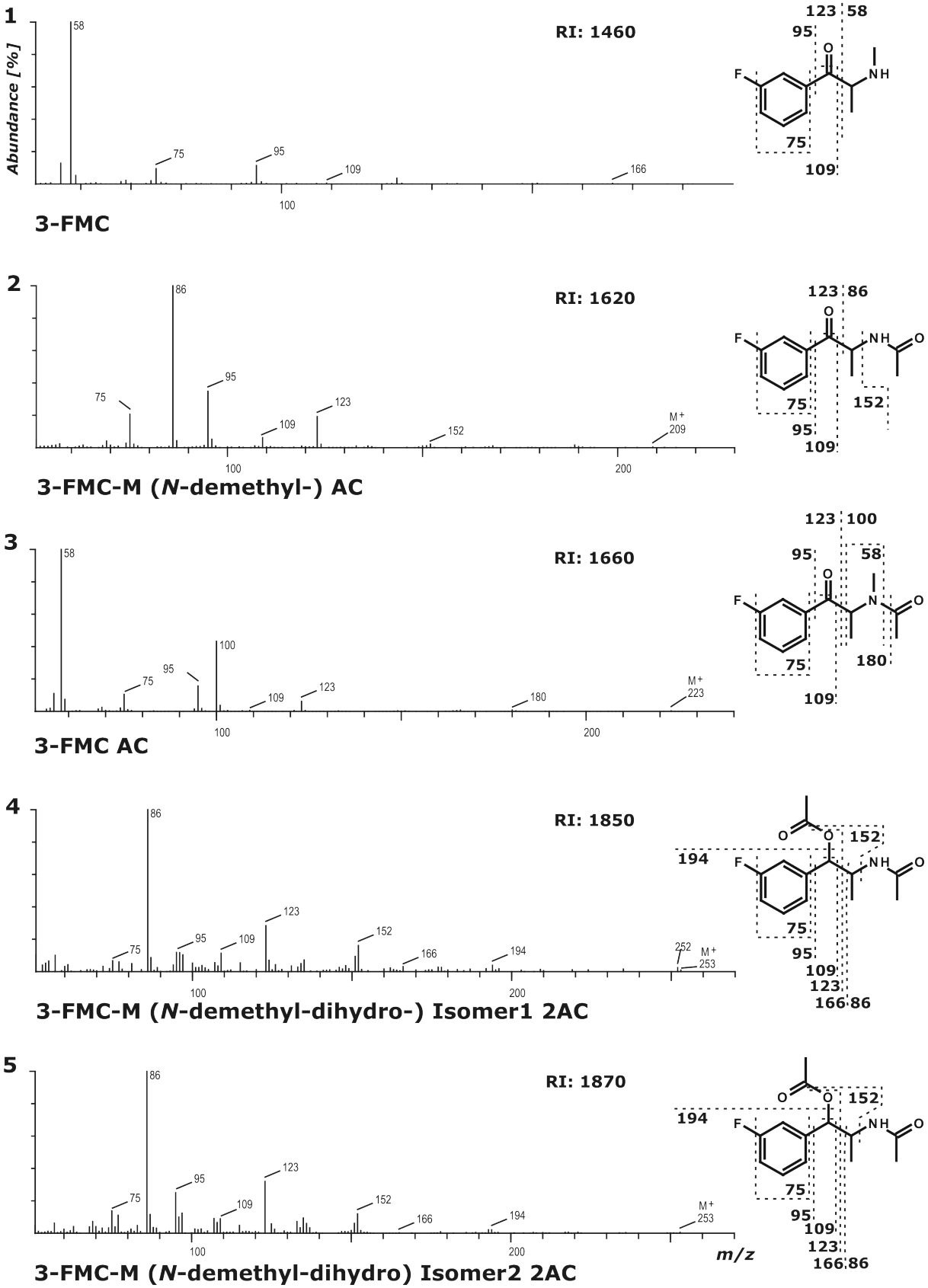

Figure 4 (a). EI mass spectra, gas chromatographic retention indices (RI), proposed structures and predominant fragmentation patterns of 3-FMC and its metabolites arranged according to their RI.

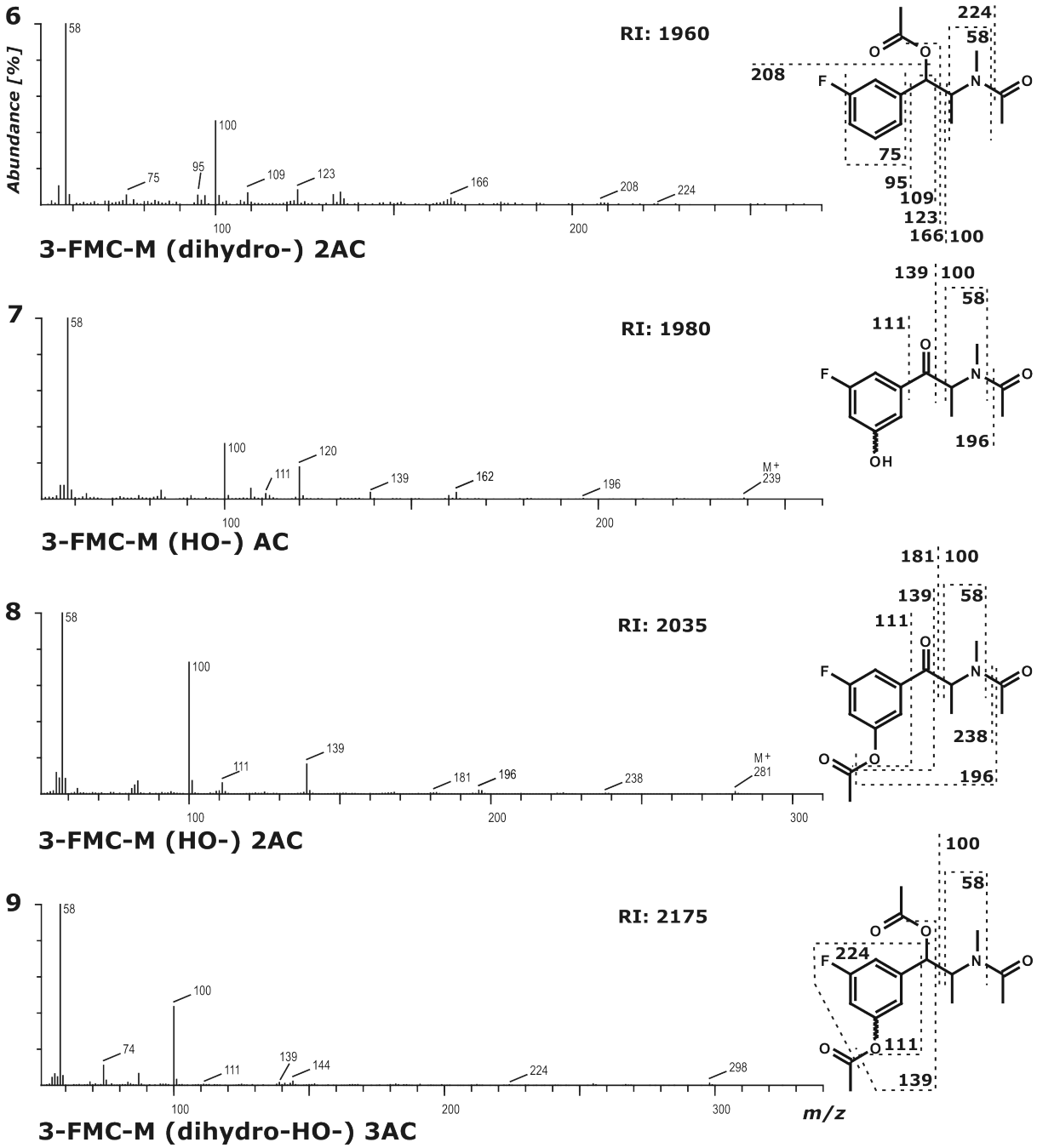

Figure 4 (b). EI mass spectra, gas chromatographic retention indices (RI), proposed structures and predominant fragmentation patterns of 3-FMC and its metabolites arranged according to their RI.

5.2 HR-ESI-MS Results

5.2.1 Confirmation of the Phase I metabolites by HR-ESI-MS

The calculated and measured molecular weights of the underivatized metabolites are shown in Table 2.

The elemental composition of all metabolites of 3-BMC and 3-FMC identified by GC-MS should be verified using the HR-ESI-MS. In addition, *N*-oxides that can be considered as precursors of the respective *N*-dealkyl compounds were detected and confirmed by characteristic fragments after HCD fragmentation, corresponding to the unchanged parent compound. It is obvious that this *N*-oxide was not detectable by GC-MS due to its thermal degradation when introduced into the GC. The calculated and measured molecular weights as well as the mass error can be found in Table 2.

Table 2. Calculated and measured exact masses and their delta values in ppm of the phase I metabolites of 3-BMC and 3-FMC using HR-ESI-MS (MS [1] scan without HCD fragmentation)

Metabolite	Modus	Calculated Mass	Measured Mass	delta (ppm)
3-^{79}BMC	MS [1]	242.0175	242.0174	-0.302
3-^{81}BMC	MS [1]	244.0154	244.0153	-0.642
3-^{79}BMC-M (*N*-demethyl-)	MS [1]	228.0018	228.0018	-0.014
3-^{81}BMC-M (*N*-demethyl-)	MS [1]	229.9998	229.9996	-0.507
3-^{79}BMC-M (*N*-demethyl-dihydro-)	MS [1]	230.0175	230.0175	0.204
3-^{81}BMC-M (*N*-demethyl-dihydro-)	MS [1]	232.0154	232.0152	-0.718
3-^{79}BMC-M (*N*-demethyl-dihydro-HO-)	MS [1]	246.0124	246.0123	-0.479
3-^{81}BMC-M (*N*-demethyl-dihydro-HO-)	MS [1]	248.0103	248.0101	-0.771
3-FMC	MS [1]	182.0975	182.0978	+1.489
3-FMC-M (N-demethyl-)	MS [1]	168.0819	168.0819	-0.052
3-FMC-M (N-demethyl-dihydro-)	MS [1]	170.0975	170.0977	0.889
3-FMC-M (dihydro-)	MS [1]	184.1132	184.1130	-0.754
3-FMC-M (HO-)	MS [1]	198.0924	198.0924	-0.068
3-FMC-M (dihydro-HO-)	MS [1]	200.1081	200.1081	0.183

5.2.2 Identification of the Phase II metabolites by HR-ESI-MS

Phase II metabolites (glucuronides or sulfates) were identified using reconstructed ion chromatograms of the calculated HR protonated molecular ions of conjugates of the identified

Phase I metabolites. The formation of the aglyca could be confirmed by comparing the corresponding MS spectra after HCD fragmentation with the MS spectra of the Phase I metabolites. Using this approach, 3-BMC-M (*N*-demethyl-dihydro-) glucuronide and 3-FMC-M (dihydro-) glucuronide could be detected at concentrations much lower than those of the unconjugated phase I metabolites. This was confirmed by comparison of the signals of the Phase I metabolites with and without conjugate cleavage. No sulfate conjugates were detected in the rat urine samples, although they are expected to be formed in humans. This will be referred to below.

5.3 Proposed metabolic pathways

From the metabolites earlier described, the following metabolic pathways can be deduced:

5.3.1 3-Bromomethcathinone

As depicted in Fig. 5, 3-BMC *N*-demethylation was observed (No. 2, 4 and 5) followed by reduction of the ketone moiety (4, 5) and adjacent ring hydroxylation (5). Metabolite 4 was also excreted as glucuronic acid conjugate (4G).

As contrast to 3-FMC, 3-BMC could not be detected in rat urine.

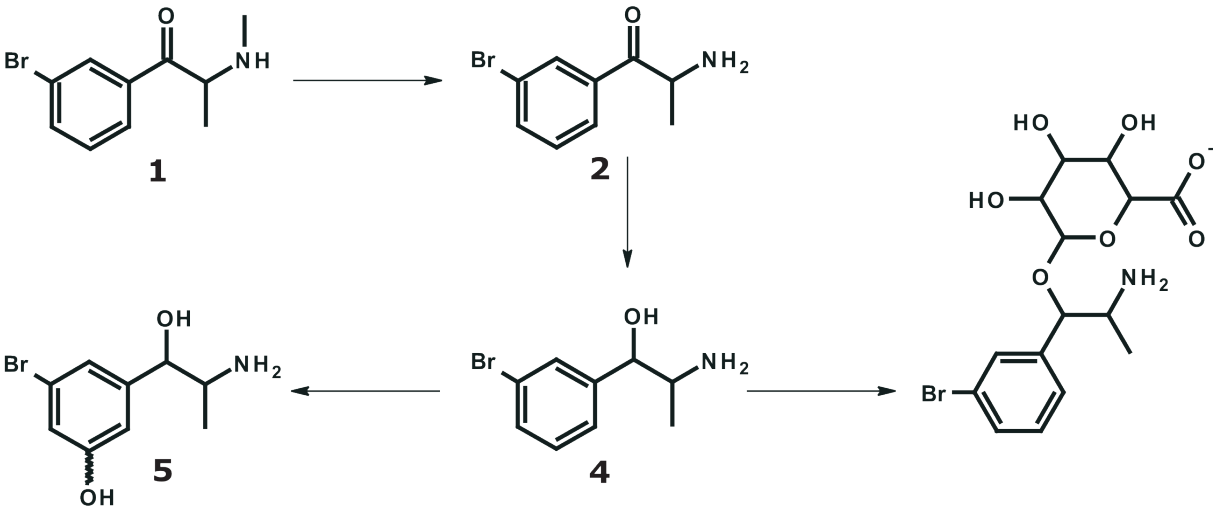

Figure 5. Proposed scheme for the Phase I and II metabolism of 3-BMC in rats (metabolite numbers correspond to the spectra numbers in Fig. 3)

5.3.2 3-Fluoromethcathinone

Concerning 3-FMC, ring hydroxylation (Fig. 6, Nos. 7, 8, 9), reduction of the beta-keto moiety (4, 5, 6, 9), *N*-demethylation (2, 4, 5) and combinations of them (4, 5, 9) were observed. In addition, the parent compound was excreted unchanged (1). Metabolite 6 was also excreted as glucuronic acid conjugate (6G).

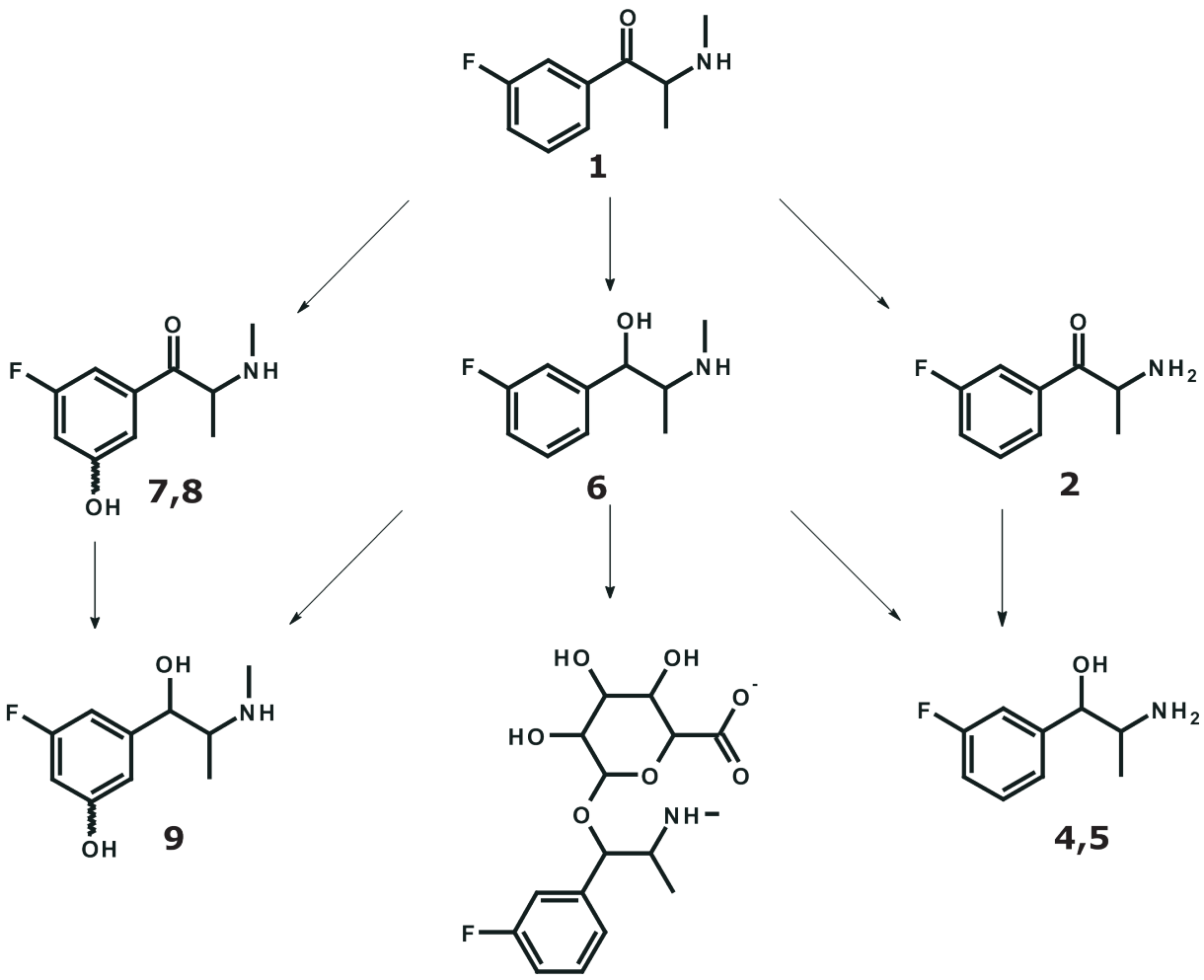

Figure 6. Proposed scheme for the Phase I and II metabolism of 3-FMC in rats (metabolite numbers correspond to the spectra numbers in Fig. 4 (a) and 4 (b))

5.4 Toxicological detection of 3-BMC and 3-FMC by GC-MS or LC-MS^n

3-BMC, 3-FMC and their metabolites were separated and identified by GC full scan EI MS after fast acidic hydrolysis, liquid-liquid-extraction and acetylation (STA) of human urine [12,14]. Mass chromatography with the following ions was used to detect the presence of 3-

BMC metabolites: *m/z* 58, 86 and 183. For detection of 3-FMC, the following ions were used: *m/z* 58, 86, 95 and 123. The most abundant metabolites of 3-BMC and 3-FMC in rat urine samples were the respective dihydro-metabolites. The identity of the peaks indicated by the selected mass chromatogram was confirmed by computerized comparison of the underlying full-scan mass spectrum with reference spectra recorded during this study. In addition, the full-scan data files acquired by the GC-MS system were evaluated by AMDIS, allowing the detection of 3-BMC and 3-FMC in prepared urine samples using the previously described procedure [19]. Also, using the previously described LC-MS^n procedure, 3-BMC and 3-FMC metabolites and the parent compound 3-FMC were detectable [26].

5.5 Enzymatic part

5.5.1 Initial CYP screening

The initial screening studies with the ten most abundant human hepatic CYPs were used to identify their ability for catalyzing the formation of the main metabolite *in vitro*. According to the supplier's advice, the incubation conditions chosen were adequate to make a statement on the general involvement of a particular CYP enzyme. The main metabolic step observed in *in vitro* incubations with recombinant CYPs was the *N*-demethylation of both 3-BMC and 3-FMC.

As shown in Fig. 7, CYP2D6, CYP2B6, CYP2C19, CYP1A2, CYP2E1 and CYP3A4 catalyzed the formation of *N*-demethyl-3-BMC, whereas CYP2B6, CYP2D6, CYP2C19, CYP2E1 and CYP3A4 were mainly capable to catalyze the demethylation of 3-FMC metabolite formation.

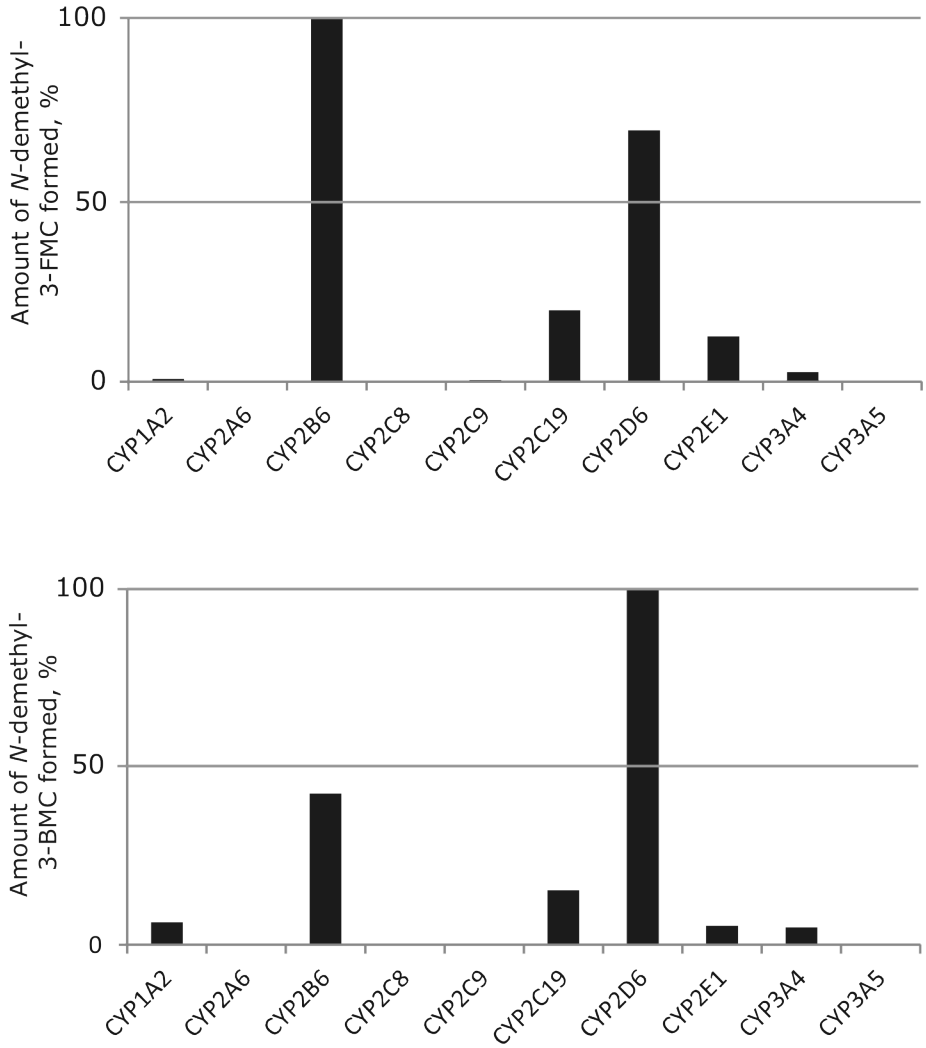

Figure 7. Relative amount of *N*-demethyl-3-FMC (upper part) and *N*-demethyl-3-BMC (lower part) formed after incubation of 250 µM each (37°C, 30 min) using the ten most important recombinant CYP isoenzymes (50 pmol/mL, each) as enzyme source.

5.5.2 Kinetic studies

The kinetic parameters could not be determined for all P450s capable of catalyzing the monitored *N*-demethylation of both substances.

Concerning 3-BMC, the kinetic profiles of CYP2D6, CYP2B6, and HLM best fit into Michaelis-Menten kinetics, as shown in Fig. 8.

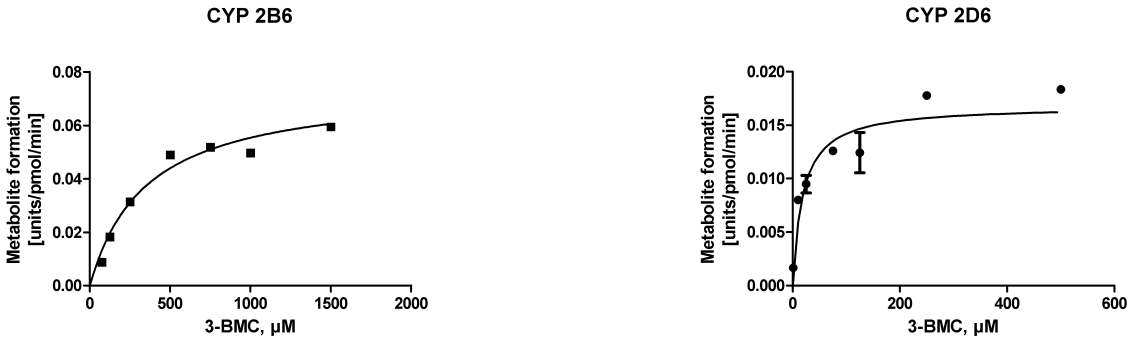

Figure 8. Enzyme kinetic plots for *N*-demethyl 3-BMC formation catalyzed by CYP2B6 (left) and CYP2D6 (right). Data points represent means and ranges (error bars) of duplicate measurements.

For 3-FMC, CYP2D6 and CYP2C19 revealed classic hyperbolic Michaelis-Menten kinetics as shown in Fig. 9, whereas CYP2B6 and HLM fitted statistically better into a biphasic kinetic model.

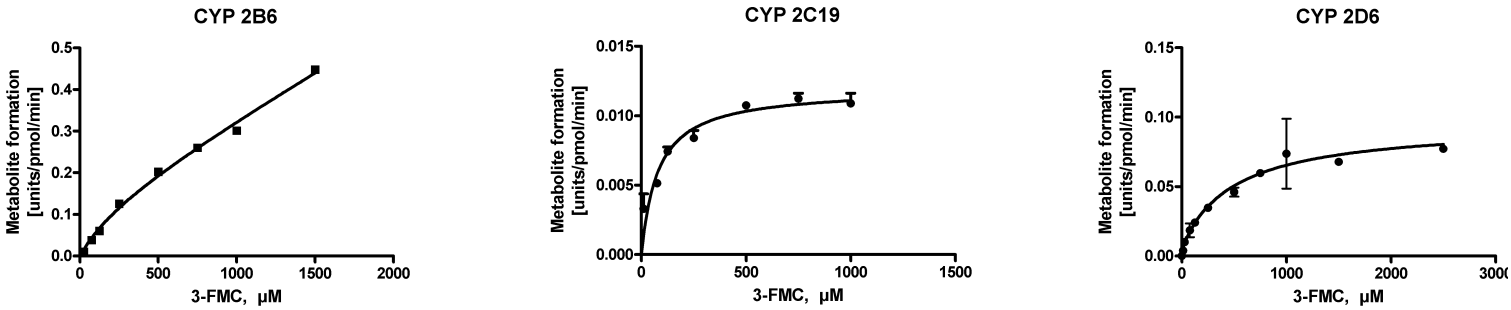

Figure 9. Enzyme kinetic plots for *N*-demethyl 3-FMC formation catalyzed by CYP2B6 (left), CYP2C19 (middle) and CYP2D6 (right). Data points represent means and ranges (error bars) of duplicate measurements.

For 3-FMC, CYP2E1 and CYP3A4, and for 3-BMC, CYP2C19, CYP1A2, CYP2E1 and CYP3A4 activities were too low for calculation of kinetic parameters. The K_m values, representing the *in vitro* affinity of the particular P450s substrates that showed sufficient activity, are listed in Table 3.

Table 3. Calculated Km values (µM)

Enzyme	K_M for *N*-demethyl-3-FMC formation	K_M for *N*-demethyl-3-BMC formation
CYP2B6	**283**[a]	**350**
CYP2D6	**12**	**18**
CYP2C19	**76**	**not determined**

[a] K_{m1}

The net clearances for particular P450s at the two substrates concentrations 1 µM and 10 µM were calculated to be, for 3-BMC, 60% / 70% and 40% / 30% for CYP2B6 and CYP2D6, respectively, and for 3-FMC, 92% / 96%, 6% / 3% and 2% / 1% for CYP2B6, CYP2D6 and CYP2C19, respectively. In conclusion, the net clearance data indicated that CYP2B6 was responsible for the main part of the total 3-BMC and 3-FMC CYP-dependent clearance, becoming even more important at higher substrate concentrations.

Comparing 3-BMC and 3-FMC kinetics, it turns out that 3-FMC metabolism underlies a partly biphasic kinetic by HLM and CYP2B6, whereas the 3-BMC data entirely showed classic Michaelis-Menten kinetics.

6.1 *In vivo* vs. *in vitro* Phase I metabolism – the role of ADH

Concerning 3-FMC, we can compare the Phase I metabolism in rats and the CYP-incubation data of human CYP enzymes to the phase I metabolism deduced from rabbit liver slice incubations by Pawlik et al. [11]. In both cases, *N*-demethylation and ring hydroxylation were initial steps.

Comparing our *in vivo* to our *in vitro* Phase I metabolism data is pointing out an interesting difference:

The results of the incubations with recombinant CYPs showed the *N*-demethylation of both 3-BMC and 3-FMC as the initial metabolic step *in vitro* whereas rat urine analysis revealed *N*-demethyl-dihydro-3-BMC and hydroxyl-3-FMC followed by *N*-demethyl-dihydro-3-FMC as the main metabolites *in vivo*. However, it should be considered that *in vivo* the alcohol

dehydrogenase should have a large impact on 3-BMC and 3-FMC reduction, which of course is not analyzed in the described *in vitro* experiments. Co-consumption of ethanol and 3-BMC or 3-FMC may lead to a prolonged half-life of these drugs of abuse and to increased plasma concentrations due to a competitive inhibition of the alcohol dehydrogenases by ethanol. The role of the ADH concerning 3-BMC and 3-BMC should be clarified by further investigations.

6.2 Phase II metabolism

For the Phase II metabolism, 3-BMC-M (dihydro-) glucuronide and 3-FMC-M (dihydro-) glucuronide could be detected. No sulfate conjugates were detected in the rat urine samples, although they are expected to be formed in humans. Concerning our screening procedures, such a difference does not really influence the detectability of both compounds. Using GC-MS, conjugates are cleaved prior to analysis, and under LC/MS^n STA conditions, the MS3 and MS2 spectra of glucuronides and sulfates are expected to be similar.

6.3 Possible CYP interactions

Concerning the kinetic studies, CYP2B6 turned out to be responsible for the main CYP-dependent clearance for both substances; becoming more important from lower to higher 3-BMC / 3-FMC concentrations. This is in line with previously published data of *N*-demethylation of amphetamine-derived compounds such as 3,4-methylenedioxymethamphetamine, MDMA and methylbenzodioxoylbutanamine, MBDB [27,28]. Therefore, it should be taken into account that interaction may be possible between strong CYP2B6 inhibitors, such as ticlopidine, and the investigated cathinone derivates leading to increased plasma concentrations and therefore severe side effects after a common dose. Additionally, genetic polymorphisms might be of relevance in some cases and should be taken into account in interpreting plasma and urine concentration of the drugs. This question should be target of further studies.

6.4 Prove of intake

The standard toxicological analysis procedure should be suitable to prove an intake of 3-BMC as well as 3-FMC.

7 REFERENCES

[1] Brandt SD, Sumnall HR, Measham F, Cole J. Analyses of second-generation "legal-highs" in the UK: initial findings *Drug Test Anal* **2010,** *2, 377, 382*

[2] R.P. Archer. Fluoromethcathinone, a new substance of abuse. *Forensic Sci Int* **2009,** *185*, 10.

[3] Anonymous Land der Traeume Forum. http://www.land-der-traeume.de/trip_lesen.php?id=8064

[4] E.E. Balint, G. Falkay, G.A. Balint. Khat - a controversial plant. *Wien. Klin. Wochenschr.* **2009,** *121*, 604.

[5] K.F. Foley, N.V. Cozzi. Inhibition of transport function and desipramine binding at the human noradrenaline transporter by N-ethylmaleimide and protection by substrate analogs. *Naunyn Schmiedebergs Arch. Pharmacol.* **2002,** *365*, 457.

[6] K.F. Foley, N.V. Cozzi. Novel aminopropiophenones as potential antidepressants. *Drug Development Research* **2003,** *60*, 252.

[7] F. Schifano, A. Albanese, S. Fergus, J.L. Stair, P. Deluca, O. Corazza, Z. Davey, J. Corkery, H. Siemann, N. Scherbaum, M. Farre', M. Torrens, Z. Demetrovics, A.H. Ghodse. Mephedrone (4-methylmethcathinone; 'meow meow'): chemical, pharmacological and clinical issues. *Psychopharmacology (Berl)* **2011,** *214*, 593.

[8] AnonymousLand der Traeume Forum. http://www.land-der-traeume.de/forum.php?t=27073&PHPSESSID=aaa914fd406db6f4232137148dad7d52)

[9] A. Winstock, L. Mitcheson, J. Ramsey, S. Davies, M. Puchnarewicz, J. Marsden. Mephedrone: use, subjective effects and health risks. *Addiction* **2011,** *106*, 1991.

[10] F. Westpfahl, T. Junge, U. Girreser, A. Jacobsen-Bauer, P. Roesner. Badesalz für die Nase - Fluormethcathinon neu auf dem Drogenmarkt. *Toxichem. Krimtech.* **2010,** *77*, 84.

[11] E. Pawlik, G. Plasser, H. Mahler, T. Daldrup. Studies on the phase I metabolism of the new designer drug 3-fluoromethcathinone using rabbit liver slices. *Int. J. Legal Med.* **2011,**

[12] H.H. Maurer, K. Pfleger, A.A. Weber, *Mass Spectral and GC Data of Drugs, Poisons, Pesticides, Pollutants and their Metabolites*, Wiley-VCH, Weinheim, **2011.**

[13] H.H. Maurer. Position of chromatographic techniques in screening for detection of drugs or poisons in clinical and forensic toxicology and/or doping control [review]. *Clin. Chem. Lab. Med.* **2004,** *42*, 1310.

[14] A.H. Ewald, D. Ehlers, H.H. Maurer. Metabolism and toxicological detection of the designer drug 4-chloro-2,5-dimethoxyamphetamine in rat urine using gas chromatography-mass spectrometry. *Anal. Bioanal. Chem.* **2008,** *390*, 1837.

[15] S.E. Clarke. In vitro assessment of human cytochrome P450. *Xenobiotica* **1998,** *28*, 1167.

[16] C.L. Crespi, V.P. Miller. The use of heterologously expressed drug metabolizing enzymes-state of the art and prospects for the future. *Pharmacol. Ther.* **1999,** *84*, 121.

[17] K. Venkatakrishnan, L.L. von Moltke, Court M.H., J.S. Harmatz, C.L. Crespi, D.J. Greenblatt. Comparison between cytochrome P450 (CYP) content and relative activity approaches to scaling from cDNA-expressed CYPs to human liver microsomes: ratios of accessory proteins as sources of discrepancies between the approaches. *Drug Metab. Dispos.* **2000,** *28*, 1493.

[18] K. Grime, R.J. Riley. The impact of in vitro binding on in vitro-in vivo extrapolations, projections of metabolic clearance and clinical drug-drug interactions. *Curr. Drug Metab* **2006,** *7*, 251.

[19] M.R. Meyer, F.T. Peters, H.H. Maurer. Automated mass spectral deconvolution and identification system for GC-MS screening for drugs, poisons, and metabolites in urine. *Clin. Chem.* **2010,** *56*, 575.

[20] H.H. Maurer, K. Pfleger, A.A. Weber, *Mass Spectral Library of Drugs, Poisons, Pesticides, Pollutants and their Metabolites*, Wiley-VCH, Weinheim, **2011.**

[21] F. Westphal, T. Junge, P. Rosner, G. Fritschi, B. Klein, U. Girreser. Mass spectral and NMR spectral data of two new designer drugs with an alpha-aminophenone structure: 4'-Methyl-alpha-pyrrolidinohexanophenone and 4'-methyl-alpha-pyrrolidino-butyro-phenone. *Forensic Sci. Int.* **2007,** *169*, 32.

[22] F.W. McLafferty, F. Turecek, *Interpretation of Mass Spectra*, University Science Books, Mill Valley, CA, **1993.**

[23] R.M. Smith, K.L. Busch, *Understanding Mass Spectra - A Basic Approach*, Wiley, New York (NY), **1999.**

[24] R.A. de-Zeeuw, J.P. Franke, H.H. Maurer, K. Pfleger, *Gas Chromatographic Retention Indices of Toxicologically Relevant Substances and their Metabolites (Report of the DFG commission for clinical toxicological analysis, special issue of the TIAFT bulletin)*, VCH publishers, Weinheim, **1992.**

[25] P. Rosner, B. Quednow, U. Girreser, T. Junge. Isomeric fluoro-methoxy-phenylalkylamines: a new series of controlled-substance analogues (designer drugs). *Forensic Sci. Int.* **2005,** *148*, 143.

[26] D.K. Wissenbach, M.R. Meyer, D. Remane, A.A. Philipp, A.A. Weber, H.H. Maurer. Drugs of abuse screening in urine as part of a metabolite-based LC-MS(n) screening concept. *Anal. Bioanal. Chem.* **2011,** *400*, 3481.

[27] M.R. Meyer, F.T. Peters, H.H. Maurer. The role of human hepatic cytochrome P450 isozymes in the metabolism of racemic 3,4-methylenedioxy-methamphetamine and its enantiomers. *Drug Metab. Dispos.* **2008,** *36*, 2345.

[28] M.R. Meyer, F.T. Peters, H.H. Maurer. Stereoselective differences in the cytochrome P450-dependent dealkylation and demethylenation of *N*-methyl-benzodioxolyl-butanamine (MBDB, Eden) enantiomers. *Biochem. Pharmacol.* **2009,** *77*, 1725.

8 ABBREVIATIONS

3-BMC	3-bromomethcathinone
3-FMC	3-fluoromethcathinone
GC-MS	gas chromatography- mass spectrometry
LC-MS	liquid chromatography- mass spectrometry
LC-HRMS	liquid chromatography- high resolution- mass spectrometry
STA	systematic toxicological analysis
IUPAC	International Union of Pure and Applied Chemistry
NMR	nuclear magnetic resonance spectroscopy
Da	Dalton

9 DANKSAGUNG

Die Dissertation entstand in der Abteilung für Experimentelle und Klinische Toxikologie der Medizinischen Fakultät der Universität des Saarlandes.

Ich danke Herrn Prof. Dr. Dr. h.c. Hans H. Maurer für die Aufnahme in seinen Arbeitskreis sowie für die zur Verfügung gestellten Materialien und Geräte. Bedanken möchte ich mich auch für die Zuversicht, die Herr Prof. Dr. Dr. h.c. Maurer mich bezüglich dieser Studie immer hat spüren lassen.

Besonderer Dank gebührt Herrn Dr. Markus R. Meyer für die Überlassung dieses interessanten Themas, die exzellente Betreuung und Anleitung sowohl während der experimentellen Phase als auch beim späteren Auswerten und Niederschreiben der Ergebnisse sowie für seine stete Diskussionsbereitschaft.

Vielen Dank auch an Frau Dr. Andrea Schwaninger für die kompetente Betreuung bei der Durchführung und Auswertung der Enzym-Versuche.

Ebenfalls möchte ich mich bei allen wissenschaftlichen und technischen Mitarbeitern der Abteilung für Experimentelle und Klinische Toxikologie für das sehr gute und konstruktive Arbeitsklima bedanken, allen voran bei Herrn Armin Weber, Herrn Golo M. Meyer, Herrn Carsten Schröder und Frau Gabriele Ulrich.

Diese Arbeit ist meinen Eltern gewidmet. Sie ermöglichen mir diese Universitätsausbildung und haben mich in allen Belangen stets unterstützt. Auch meine Geschwister, meine Freundin und meine Freunde, darunter vor allem Benedikt Müller, haben großen Anteil an der Fertigstellung dieser Arbeit. Vielen Dank für die wertvolle Unterstützung und Geduld.